IEEE Photonics Journal
An IEEE Photonics Society Publication

Open Access

Scalable Wideband Principal Component Analysis via Microwave Photonics

Volume 8, Number 2, April 2016

Thomas Ferreira de Lima
Alexander N. Tait
Mitchell A. Nahmias
Bhavin J. Shastri, Member, IEEE
Paul R. Prucnal, Fellow, IEEE

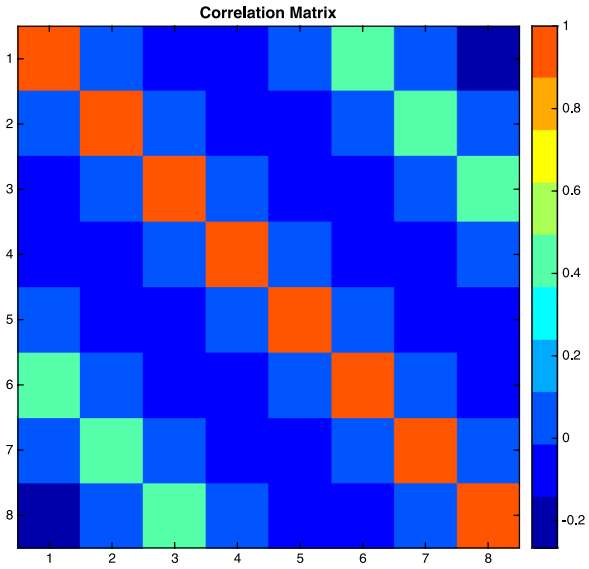

DOI: 10.1109/JPHOT.2016.2538759
1943-0655

IEEE photonics SOCIETY

IEEE

Scalable Wideband Principal Component Analysis via Microwave Photonics

Thomas Ferreira de Lima, Alexander N. Tait, Mitchell A. Nahmias, Bhavin J. Shastri, *Member, IEEE*, and Paul R. Prucnal, *Fellow, IEEE*

Lightwave Communications Research Laboratory, Department of Electrical Engineering, Princeton University, Princeton, NJ 08544 USA

DOI: 10.1109/JPHOT.2016.2538759

Manuscript received December 2, 2015; revised February 28, 2016; accepted March 1, 2016. Date of publication March 4, 2016; date of current version March 21, 2016. This work was supported by Lockheed Martin Corporation under Award 4101916239. Corresponding author: T. Ferreira de Lima (e-mail: tlima@princeton.edu).

Abstract: Microwave photonics (MWP) provides advantages in bandwidth performance and fan-in scalability that are far superior to electronic counterparts. Processing of many channels at high bandwidths is not easily achievable in any electronic implementation. We consider an MWP system that iteratively performs principal component analysis (PCA) on partially correlated, eight-channel, and 13-GBd signals. The system that is presented is able to adapt to oscillations in interchannel correlations and follow changing principal components. Wideband multidimensional techniques are relevant to > 10-GHz radio systems and could bring solutions for intelligent radio communications and information sensing.

Index Terms: Microwave photonics signal processing, optical neural systems, radio frequency (RF) photonics, information processing.

1. Introduction

Principal component analysis (PCA) is a well-known technique for pattern recognition and dimensionality reduction for multidimensional random variables. It is the basis for many statistical analyses that rely on multivariate correlations [1]. We interest ourselves in the spatial correlation of multiple time series, particularly radio frequency (RF) signals.

PCA and its cousin statistical procedures, such as independent component analysis (ICA), are a fundamental part of the solution to the blind source separation (BSS) problem in RF signal processing [2], which is a useful technique for spectrum sensing in cognitive radio systems [3]. The arrayed-antenna system design used to solve BSS bears a fatal challenge to digital signal processing (DSP): the marriage between high bandwidth and large fan-in. Phased-array antenna systems are common for millimeter-wave RF frequencies, e.g., 24, 40, 60, and 77 GHz, wherein each transmission band support multi-gigabit/s data rates. Conventional beamforming techniques rely on digital signal processors to optimize weights and phase delays that multiply signals coming from each antenna. However, baseband processors (which include analog-to-digital converters) at these bandwidths are costly and complex. Hence, a method for carrying out these operations before digitization is warranted.

Summation of many channels (fan-in) at high bandwidths is not easily achievable in any electronic implementation, as a result of inherent bandwidth and capacitive limitations of this platform. Recently, a 16-channel, 60 GHz analog beamformer was demonstrated, but it relies on

combining RF signals two by two at every stage [4]. This is the primary bottleneck that is addressed in this paper with a photonic hardware approach. Emerging technologies that surpass the performance allowed by physical limits of semiconductors, such as rapid single flux quantum (RSFQ), based on cryogenically refrigerated superconductors, are expected to perform at most at hundreds of GHz [5]. On the other hand, optical telecommunication systems reliably operates on the C-band, which holds ~5 THz of available bandwidth capacity, at room temperature.

Recent developments in photonic integration will allow large, complex networks that utilize this bandwidth to exist on a single chip. Wavelength-division multiplexing (WDM) can create spectrally narrow channels at different wavelengths that are multiplexed simultaneously onto a single optical waveguide. Therefore, microwave photonics (MWP), equipped with WDM, is exceptionally suitable for the parallel processing of many RF signals, in particular the spectrum belonging to SHF (3–30 GHz) and the lower part of EHF (30–300 GHz) as classified by the International Telecommunications Union (ITU), which include wireless LAN (local area network), radar, communication satellites, and television broadcasting.

Furthermore, MWP brings additional advantages relative to electronic microwave systems, combining low loss, high bandwidth, tunability, and immunity to electromagnetic interference. Because fast response times are inherent to photonics, MWP systems possess ultrafast (microsecond) tunability, which add the capability to adapt to signals in real-time. Moreover, since wideband signals possess a bandwidth that is just a fraction of optical frequencies, MWP systems offer true-time delays with typical ~ns tunability range, as opposed to frequency-dependent RF phase-shifters. This implies that the same MWP device can process signals traveling either in the 10 GHz band (ultra-wideband) or in the 60 GHz band (millimeter-wave), whereas analog RF beamformers have to be designed to work specifically in a narrow range of the RF spectrum.

For these reasons, MWP attracted great interest for its applications in arbitrary waveform generation, chirped microwave pulse generation, microwave differentiators, and real-time operations over microwave signals [6], but few present the advantages of tunability or wavelength-division multiplexing (WDM). Recent work [7] demonstrated weighted addition of WDM optical signals (8 channels, 1 Gbaud each), showcasing iterative PCA.

In this paper, we demonstrate an MWP implementation of iterative PCA for 8-channel, 13 Gbaud RF signals and show a novel technique for continuously controlling their correlation matrix. We improve on [7] by operating at much higher fan-in × bandwidth capacity (beyond what is achievable by digital signal processors) and controlling spatial correlations between signals using higher-order Markov chains. We show that this system performs well under these conditions, opening up PCA to the SHF band. Such a device, when combined with a real-time PCA controller, could be essential as a front-end to high-performance DSP systems, extracting principal components from multi-dimensional systems while adapting to correlation changes in the microsecond timescale.

2. Methods

The experimental testbed is separated into three sections: input generator; weighted addition; and feedback control (see Fig. 1). In this article, we show a 13 Gbaud, eight-channel WDM input generation circuit that allows for seven-parameter control of inter-channel correlations. An electric non-return-to-zero (NRZ) signal with several GHz bandwidth is constructed using a single pulse-pattern generator (PPG) carrying a programmable 8192-long bit pattern. Although we use NRZ signals for testing, we treat them as analog waveforms throughout the experiment. This signal is imprinted in 16 wavelength carriers via a Mach-Zehnder modulator (MZM), which output complementary polarities at each arm. 16 wavelengths are necessary to encode eight channels with both polarities (positive and negative) [see Fig. 3(a)]. This scheme enables the possibility of effectively *negative weighting* via optical attenuation only. At no time do corresponding positive and negative wavelengths have attenuations that are both nonzero. After modulation, an equally-spaced fiber Bragg grating (FBG) array adds wavelength-dependent time-of-flight delays so that each successive channel is one nanosecond delayed with respect

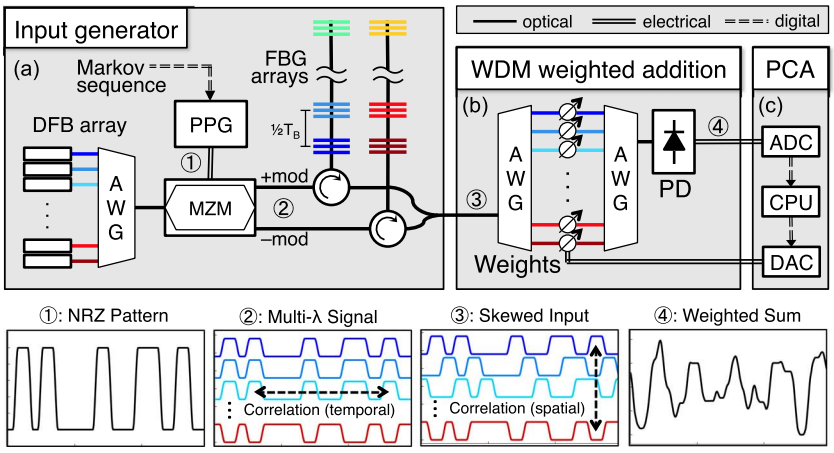

Fig. 1. Experimental setup, adapted from [7]. (a) Input generator, where DFB is the distributed feedback laser; AWG is the athermal arrayed-waveguide grating multiplexer with 200 GHz (1.6 nm) channel spacing; PPG is the 13 Gbaud pulse pattern generator; MZM is the 20 GHz Mach-Zehnder modulator; FBG stands for fiber Bragg grating. (b) WDM weighted addition where circles are variable optical attenuators with transmission windows matched with the AWG, and PD: 28 GHz photodiode. (c) PCA algorithm, where ADC is the analog-digital converter with effective 100 GS/s and 32-bit precision; CPU is the central processor; DAC is the digital-analog converter. The PD+ADC system is essentially an optical sampling module of a high-bandwidth sampling scope, which communicates to the CPU via a GPIB link. Illustrations show signals at various points in the circuit: ① RF input to the system that exhibits temporal autocorrelation. ② Modulated WDM optical signals—complementary modulations are provided by the MZM. ③ λ-dependent delays transform initial temporal correlation into instantaneous spatial correlations. ④ electrical output of the PD representing the weighted sum of correlated channels.

to each other [see Fig. 3(a)]. This fixed delay is instrumental in transforming temporal correlation of the NRZ sequence into spatial correlations [see Fig. 1: ② and ③; and (2)]. Another function of the FBG array is to select 8 wavelengths corresponding to positive or negative modulations of respective channels (Fig. 1(a): ① and ②). The weighted addition circuit is very similar to a finite impulse response (FIR) microwave photonic filter (cf. [6]) but with a wavelength-dependent tunable weight bank (Fig. 1). Here, the weight bank weights each channel independently and a single photodetector (PD) performs the desired *weighted addition* by carrying out optical-to-electrical conversion (Fig. 1(b): ③ and ④). A CPU connected to the setup [see Fig. 1(c)] has the capability of recording and storing these signals to perform calculations. Software has been developed to analyze the signals and perform singular value decomposition (SVD) or iterative PCA algorithms by providing feedback control of the weight bank.

PCA linearly transforms a set of N variables $x_i(t)$, with $i = 1, \ldots, N$, into a set of principal components (PCs) devoid of second-order correlations, i.e., $\langle \tilde{x}_i \cdot \tilde{x}_j \rangle_t = 0$. In order to study the performance of a wideband PCA algorithm, one needs to reliably generate partially correlated input signals with continuous control. We explain next how one can use the programmability of the NRZ signal and the fixed inter-channel delays to continuously control the correlation between channels. Assume that the bit sequence takes the form $X(n) \in \{-1, 1\}$. Each channel carries a copy $X_k(n)$ of the bit pattern $X(n)$ but shifted by 1 ns $\pm$ 5 ps slots of time [see (1)]. In order to lay an integer number of bits per slot, the PPG bit rate is set to a multiple of 1 Gbaud, say d Gbaud, i.e., d bits per nanosecond. The inter-channel correlation can be calculated as follows:

$$X_{k+1}(n + kd) = X_1(n) \equiv X(n) \tag{1}$$

$$\begin{aligned} \langle X_i(n), X_j(n) \rangle &= \langle X(n - (i-1)d), X(n - (j-1)d) \rangle \\ &= \langle X(n'), X(n' + (i-j)d) \rangle \end{aligned} \tag{2}$$

$$\begin{aligned} \Sigma_{ij} &\equiv \mathbb{E}\big(\langle X_i(n), X_j(n) \rangle\big) \\ &= \mathbb{E}(\langle X(n), X(n + |i-j|d) \rangle) \equiv K(|i-j|) \end{aligned} \tag{3}$$

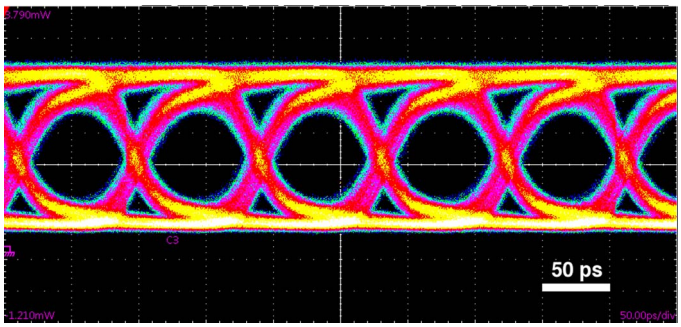

Fig. 2. Eye diagram of an unweighted 11 Gbaud NRZ signal at the output of the setup (see Fig. 1. ④). The photodiode noise level is at 10 μW over a maximum power input of 5 mW, limiting the sampling precision to 9 bits. The signal-to-noise ratio was measured as 11 dB.

where $\langle \ldots \rangle$ represents an inner product averaged over all n. Equation (2) shows that a *spatial correlation* can be seen as a *temporal correlation* (see Fig. 1.③). In addition, (3) shows that the correlation matrix element Σ_{ij} only depends on the distance $|i-j|$: such matrices are called *symmetric Toeplitz matrices*. It is necessary to program the bit sequence such that we can control the correlation $K(|i-j|)$ in (3) for $|i-j| \in \{1,\ldots,m\}$—evidently, $K(0) = \langle X(n), X(n)\rangle = 1$. To achieve this, the NRZ bit pattern is defined by an additive Markov-chain (MC) sequence of order m and dimension d [defined by (4)]

$$\mathbb{P}(X(n) = 1 | X(n-d), \ldots, X(n-(m-1)d)) = \sum_{k=1}^{m} f(X(n-kd), k) \tag{4}$$

$$\Longrightarrow K(r) = \sum_{r'=1}^{m} F(r') K(|r-r'|) \forall\, r \geq 1, \text{ where } F(r) = f(1,r) - f(-1,r). \tag{5}$$

The additive property of the MC sequence can be understood as a probability of the current number being linearly dependent on the set of samples in the past, hence the sum in (4). The result in (5) is demonstrated in [8], where $F(r)$ is referred to as *memory function*. Its recursive definition results is rather intuitive: for example, correlation between channels 3 and 1 depends directly on $F(2)$, but since the correlation between channels 3 and 2 (and also between 2 and 1) is related by $F(1)$, then correlation between channels 3 and 1 also have an "indirect" dependence on $F(1)^2$.

For this study, we chose $m = 7$ and bit rates $d = 1,\ldots,13$ Gbaud—our PPG circuit is limited to 13 Gbaud. The symmetric Toeplitz matrix Σ has the property of having eight positive eigenvalues $(E_i; i = 1,\ldots,8)$, corresponding to the variances of the PCs; and eight symmetric or anti-symmetric orthogonal eigenvectors, corresponding to the respective eight weight vectors $\boldsymbol{\mu}_i$—also called principal component coefficients—that decompose signals $\boldsymbol{x}(t)$ into the i-th PC $\tilde{x}_i(t) = \boldsymbol{\mu}_i \cdot \boldsymbol{x}(t)$. These PCs can be calculated by power iteration methods or SVD. Iterative methods recursively multiply the signals by their correlation matrix $(\Sigma^n x(t))$ until the component with the greatest eigenvalue trumps the others. The ratio between the first and second eigenvalue of Σ—$R \equiv E_1/E_2$—is thus a natural figure of merit for the analysis of convergence rates; i.e., the greater R, the more "prominent" the first PC is with respect to all others. In this work we discovered that a memory function with $m = 7$ parameters provide enough diversity of PC coefficients to be tested.

Having described the partially-correlated, multi-channel NRZ sequence as input, we proceed to describe the PCA algorithm. Its goal is to control the weight bank so that it outputs the first principal component of this multidimensional signal. The algorithm is divided in two steps.

First, the CPU digitizes and stores in memory each of the eight channels waveforms by individually selecting them using the filter bank.

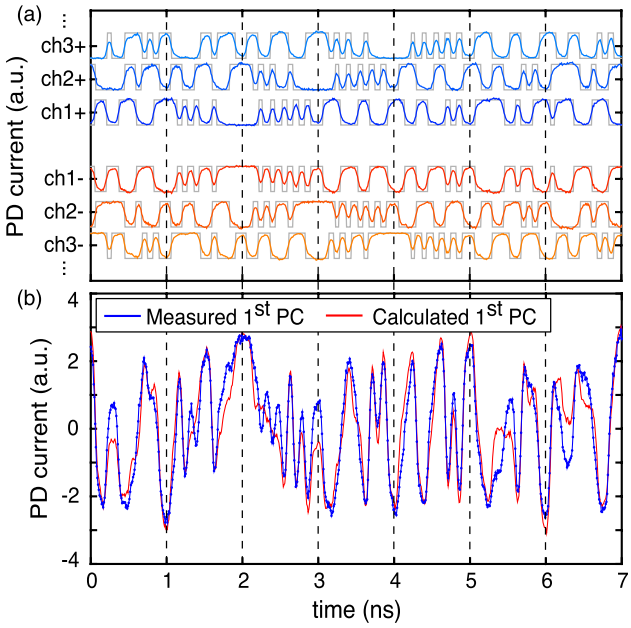

Fig. 3. Example of a PCA task on a 13 Gbaud bit pattern yielding 93% accuracy (cf. caption of Fig. 4). (a) Modulated waveforms before the weight bank (see Fig. 1.③). Note the delay of 1 ns between subsequent channels. We show only three of the eight channels for clarity purposes. The distortion from the MC bit pattern (gray) arises from the bandwidth limitation in the PPG circuit. (b) After completion of PCA task, the measured first PC waveform (see Fig. 1.④) is compared to the SVD-calculated one.

In the second step, we simulate an iterative weight control algorithm called normalized Hebbian learning rule, described in (6), [7], and [9]. We chose an iterative algorithm because it allows for an online method that learns and self-adjusts for changes in inter-channel correlations over time [9], [10]

$$\begin{aligned}\Delta\boldsymbol{\mu}_1 &= \gamma\left\langle \boldsymbol{x}(t)\boldsymbol{\mu}_1 \cdot \boldsymbol{x}(t)\right\rangle_t \\ &= \gamma\left\langle \boldsymbol{x}^T(t)\boldsymbol{x}(t)\right\rangle_t \cdot \boldsymbol{\mu}_1 \approx \gamma\Sigma \cdot \boldsymbol{\mu}_1 \\ \boldsymbol{\mu}_1 &\leftarrow \frac{\boldsymbol{\mu}_1 + \Delta\boldsymbol{\mu}_1}{\|\boldsymbol{\mu}_1 + \Delta\boldsymbol{\mu}_1\|}.\end{aligned} \tag{6}$$

The algorithm only requires a sample of the output waveform after weighted addition—which is carried out by the ADC with a time window corresponding to 2000 bits—and its correlations with the stored waveforms samples. After a finite number of iterations, $\boldsymbol{\mu}_1$ in (6) converges successfully to the first PC. In this experiment, the iteration count was limited to 40, when the converged weight value is compared with the PC computed by the SVD method. This algorithm can be trivially extended to calculate the other PCs. In this setup, the CPU is responsible for all correlation computations, and therefore limits the control loop latency—or convergence rate. Ideally, a field-programmable gate array (FPGA), or an electronic circuit connecting photodetectors and weights can provide a much faster convergence rate—on the order of MHz [10].

In the prototype experiment [7], electronic non-idealities caused the accuracy of the PCA algorithm to suffer: RF amplifiers that provided the necessary gain between the PPG and the MZM, and between the PD and the ADC (not shown in Fig. 1) were band limited to 1.3 GHz. Impedance mismatch was also present in the circuit, introducing overshoot and ringing. These obstacles were overcome by replacing the MZM gain circuit with a 12.2 Gbit/s optical modulator driver and the PD+ADC system with a high-frequency optical sampling module (see caption of Fig. 1). The modulator driver was operated with low gain so that the output was small compared to the V_π of the MZM. EDFAs produced necessary optical amplification to keep signals above noise floor of the filter bank and the photodetector.

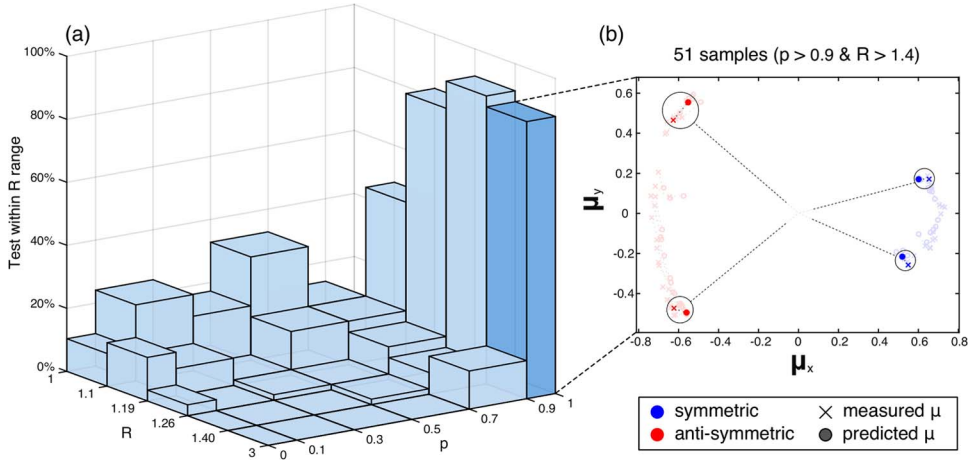

Fig. 4. Accuracy analysis of 290 runs of the experimental PCA task. (a) Histogram relating the accuracy p (square of dot product between predicted and measured PC weight vector) and R ratio between the first and second eigenvalues. The histogram was binned according to quintiles of R—each bin contains many different Markov memory functions mapping to the same range of R. The experimental PCA task accurately $(p > 0.9)$ converges to the correct weight for $R > 1.2$, which translates to the first PC being 20% more "prominent" than the second PC. Low accuracy can be explained by lack of convergence or convergence to the wrong PC. (b) 51 weight vectors contained in the rightmost bin (darker blue) of the histogram in (a). Four examples were highlighted for clarity. The weight vectors were projected onto a convenient plane that highlights the spatial diversity of the explored weight vectors generated by different Markov parameters.

However, new obstacles arose at the 10 Gbaud mark. Two effects can cause the experimental waveform to deviate from the MC bit sequence [see Fig. 3(a)]: low-pass filtering in electronic circuitry of the PPG and unwanted delay mismatch between channels across the optical circuit. We found that, although the first effect distorts the waveforms significantly, it does not ultimately change the first PC weights. The second effect, however, can effectively cause inter-channel partial correlations to disappear. For example, for $d = 10$ GHz, the bit period is 100 ps, corresponding to 2 cm of standard single-mode fiber (SSMF). A delay of 50 ps (or 1 cm in fiber) would overlap neighboring bits, thereby erasing intended correlation between channels. The second effect was minimized in this setup by fine-tuning delay lines across all channels.

3. Results

First, it is necessary to evaluate the characteristics of the input signal. NRZ waveforms are useful for analyzing noise and bandwidth. Fig. 2 shows that the NRZ waveforms are properly modulated onto wavelength carriers and back to photocurrents with sufficiently high signal-to-noise ratio. In Fig. 3(a), we present the intended NRZ bit pattern at a 13 Gbaud bit rate overlapped by the waveform generated by the PPG. Since the PPG is operating at maximum speed, one can observe the effects of low-pass filtering at the measured signals. However, as previously mentioned, the signals are still strongly correlated with PC vectors close to the originally calculated by the Markov chain method. After a multichannel signal with partial spatial correlations is generated, the PCA iterative algorithm consistently converges to the well-defined first PC. Therefore, we have a good correlation between our high bandwidth online PCA approach and an optimal offline approach [see Fig. 3(b)]. Note that in this case, the converged output signal and the SVD-predicted one follow each other without visible low-pass filtering. This illustrates the fact that each channel in the weight bank [see Fig. 1(b)] has a flat top pass band of ~100 GHz, much higher than the currently tested 13 Gbaud.

The necessary key to reveal each of the eight PCs of an eight-dimensional RF signal is a weight vector of dimension 8. Finding this key is the fundamental objective of PCA: If the correlation changes, the key changes. In this study, we generated an unbiased binary additive

Markov sequences of seventh order $(m = 7)$, as described in (4). From the memory function $F(r)$ used to create such a sequence, we can mathematically predict the inter-channel correlation values $K(r)$ and the matrix Σ, and therefore the expected "PC" eigenvectors $\boldsymbol{\mu}_i$. Fig. 4(b) shows that the weight vectors found by the iterative algorithm match the predicted ones to great accuracy. A great number of memory functions were used to generate a continuous trace of PC coefficients in order to demonstrate that the experiment can handle arbitrary weight vectors. The setup can therefore reverse engineer the key to the first PC of the input signals in less than 40 iterations. That key is only dependent on the partial correlation of input signals—not dependent, notably, on the bit rates of the individual signals themselves: the system performs equally well for NRZ patterns of 1 Gbaud and 13 Gbaud, suggesting that it can go well beyond the NRZ signal generation capabilities. In addition, we observe that performance does not depend on the orientation of the PC coefficients. It only depends on the magnitude of R [see Fig. 4(a)].

The presence of noise and the inexact command of effective weight in the weight bank prevent the system from achieving perfect close-to-100% accuracy for all R [see Fig. 4(a)]. The former stems mostly from the electronic components, since we observed that thermal noise overwhelms amplified spontaneous emission (see Fig. 2). The latter, more important, can cause convergence to a different PC or to a linear combination of PCs in cases where R (see Fig. 4). Both effects can be minimized by integrating the system onto an optoelectronic chip, with less polarization drift; less variability across WDM channels; and more precise controls over filters and cross-saturation [11].

4. Discussion

Previous work in MWP filtering [6], beamforming [12], and cognitive radio [2] has included high-bandwidth analog signal processing. However, they lack control algorithms that could adapt to changing environments, which is necessary for online analysis. In particular, one can expect the partial correlations of signals coming from an antenna array to drift over time. In the cognitive radio BSS context, e.g., this can be caused by moving sources. Thus, the circuit has to learn and self-adjust to these new conditions—a task performed by the PCA module shown in Fig. 1. As a result, it is imperative that the online PCA task is solved by iterative methods rather than offline methods such as SVD.

The time it takes for one iteration of the algorithm is limited primarily by the acquisition time of the sampling scope and serial I/O from the CPU. Implementing the controller with an embedded real-time system that consists of a wideband ADC and FPGA logic could therefore greatly reduce convergence time. Here, the Hebbian learning rule used 2000 NRZ bits at each iteration step, which corresponds to 0.2 μs at 10 Gbaud. If a controller could update the weights each 0.2 μs, then the system would converge in at most 40 steps, or 8 μs, over which we assume that the inter-channel correlation stayed constant. The convergence rate can be increased if R is large enough $(R > 1.2)$. A short convergence time demonstrates that optoelectronic circuits can be used to follow non-stationary PCs in real-time [10]. This convergence time is important for dealing with moving sources in phased-array systems.

In a phased-array transceiver, signals are delayed with respect to each other and may suffer from multipath interference or loss of line-of-sight, especially in millimeter-wave wireless systems. To counter these, orthogonal-frequency division multiplexing (OFDM) is often used [13]. The baseband frequency is channeled in such a way that can be accommodated by the bandwidth of ADCs and digital electronic circuits, typically under 1 GHz [14]. Therefore, there will be a correlation between signals received by the antennas due to the spatial coherence of the travelling wave. A real-time principal component analyzer will be sensitive to these correlations.

In contrast to standard DSP, the WDM approach offers the possibility to scale fan-in without severely jeopardizing bandwidth in the weighted addition operation. The C-band and L-band combined could support simultaneous transmission and passive *weighting* of 200 channels operating at ~10 GHz each [15], [16]. A single PD performs *addition* by transforming total optical power of all channels into photocurrent. The final optoelectronic circuit for first PC extraction

requires one modulator and one filter per channel and one PD, all with the same bandwidth requirement as each of the input channels. Here, the modulator and PD ultimately impose the bandwidth limitation of each channel. We note, however, that commercially available components offer tens of GHz of bandwidth.

In the real-time example above the bandwidth requirement for the PD would be 10 GHz. A statistical evidence window of ~2000 bits would impose a maximum feedback latency of 0.2 μs on the PCA control circuit. This leaves enough room for 8-bit ADCs clocked at 500 MHz and FPGA logic gates executing Oja's rule and driving the variable optical attenuators.

5. Conclusion

We have demonstrated how a WDM-based MWP system can be used to find and follow principal components of wideband, multidimensional RF signals. The present work introduced a novel methodology to continuously control partially correlated wavelength-carried signals using additive Markov chains. We showed that the iterative normalized Hebbian rule allows for a type of unsupervised learning—in this case, learning the first principal component of a multichannel signal—which can be extended to a real-time version. Although a more thorough analysis will require faster electronic sources, we showed that photonics provide high-fidelity in carrying wideband RF waveforms. Further work will focus on the integration; on the acceleration of control loop latency to allow for faster convergence; on the generation of faster aperiodic partially correlated analog signals; and on the fundamental limitations imposed by inexact weight command and noise.

Future RF processing will demand wideband and intelligent systems, combining high-fan-in and high-bandwidth. Neuromorphic approaches to optical computing have attracted renewed interest [17]–[20], and can potentially offer an outlet to this demand. In that context, PCA-based learning may provide tools for cognitive radio, spectrum sensing, and other areas of RF processing.

This work may also find application for blind source separation in multi-antenna systems. Arrayed-antenna systems in particular often digitizes largely redundant multidimensional signals [21]. MWP-based PCA simultaneously brings dimensionality reduction, feature extraction, and learning capabilities to analog processors, reducing strain on digital signal processing requirements in wideband RF systems. That is, one baseband processor would be required to digitize and process one principal component rather than the original eight-dimensional input—an eight-fold reduction. We estimate that a device like this is an essential front-end to DSP systems with a large number of high-bandwidth inputs.

References

[1] I. T. Jolliffe, *Principal Component Analysis*, 2nd ed. New York, NY, USA: Springer-Verlag, 2002.
[2] M. Baylor, D. Z. Anderson, and Z. Popovic, "Holographic blind source separation at radio frequencies," presented at the Photorefractive Effects, Photosensitivity, Fiber Gratings, Photonic Materials More, Squaw Creek, CA, USA, 2007, Paper TuB1.
[3] N. T. Khajavi, S. Sadeghi, and S. M.-S. Sadough, "An improved blind spectrum sensing technique for cognitive radio systems," in *Proc. 5th Int. Symp. Telecommun.*, 2010, vol. 4290, pp. 13–17.
[4] A. Natarajan *et al.*, "A fully-integrated 16-element phased-array receiver in SiGe BiCMOS for 60-GHz communications," *IEEE J. Solid-State Circuits*, vol. 46, no. 5, pp. 1059–1075, May 2011.
[5] M. J. Rodwell, *High-Speed Integrated Circuit Technology: Towards 100 GHz Logic*. River Edge, NJ, USA: World Scientific, 2001.
[6] J. Capmany *et al.*, "Microwave photonic signal processing," *J. Lightw. Technol.*, vol. 31, no. 4, pp. 571–586, Feb. 2012.
[7] A. N. Tait, J. Chang, B. J. Shastri, M. A. Nahmias, and P. R. Prucnal, "Demonstration of WDM weighted addition for principal component analysis," *Opt. Exp.*, vol. 23, no. 10, pp. 12758–12765, May 2015.
[8] S. S. Melnyk, O. V. Usatenko, V. A. Yampol'skii, S. S. Apostolov, and Z. A. Maiselis, "Memory functions and correlations in additive binary Markov chains," *J. Phys. A, Math. Gen.*, vol. 39, no. 46, pp. 14289–14301, Nov. 2006.
[9] E. Oja, "A simplified neuron model as a principal component analyzer," *J. Math. Biol.*, vol. 15, no. 3, pp. 267–273, Nov. 1982.
[10] T. Ferreira de Lima, A. N. Tait, B. J. Shastri, M. A. Nahmias, and P. R. Prucnal, "Proposal for CMOS-compatible optoelectronic integrated circuit for online wideband PCA," in *Proc. IEEE SUM Ser.*, Jul. 2015, vol. 2, pp. 97–98.

[11] A. N. Tait, T. Ferreira de Lima, M. A. Nahmias, B. J. Shastri, and P. R. Prucnal, "Continuous calibration of microring weights for analog optical networks," *IEEE Photon. Technol. Lett.*, vol. 28, no. 8, pp. 887–890, Apr. 2016.
[12] J. Chang, M. P. Fok, R. M. Corey, J. Meister, and P. R. Prucnal, "Highly scalable adaptive photonic beamformer using a single mode to multimode optical combiner," *IEEE Microw. Wireless Compon. Lett.*, vol. 23, no. 10, pp. 563–565, Oct. 2013.
[13] P. Smulders, "Exploiting the 60 GHz band for local wireless multimedia access: Prospects and future directions," *IEEE Commun. Mag.*, vol. 40, no. 1, pp. 140–147, Jan. 2002.
[14] C. S. Choi *et al.*, "60-GHz OFDM systems for multi-gigabit wireless LAN applications," in *Proc. 7th IEEE CCNC*, 2010, pp. 1–5.
[15] J. Yamawaku *et al.*, "Simultaneous 25 GHz-spaced DWDM wavelength conversion of 1.03 Tbits (103×10 Gbits) signals in PPLN waveguide," *Electron. Lett.*, vol. 39, no. 15, pp. 1144–1145, Jul. 2003.
[16] E. Yamada *et al.*, "106 channel 10 Gbit/s, 640 km DWDM transmission with 25 GHz spacing with supercontinuum multi-carrier source," *Electron. Lett.*, vol. 37, no. 25, pp. 1534–1536, Dec. 2001.
[17] J. Hasler and B. Marr, "Finding a roadmap to achieve large neuromorphic hardware systems," *Frontiers Neurosci.*, vol. 7, no. 7, p. 118, Sep. 2013.
[18] M. A. Nahmias, B. J. Shastri, A. N. Tait, and P. R. Prucnal, "A leaky integrate-and-fire laser neuron for ultrafast cognitive computing," *IEEE J. Sel. Topics Quantum Electron.*, vol. 19, no. 5, Sep./Oct. 2013, Art. no. 1800212.
[19] M. A. Nahmias, A. N. Tait, B. J. Shastri, T. F. de Lima, and P. R. Prucnal, "Excitable laser processing network node in hybrid silicon: Analysis and simulation," *Opt. Exp.*, vol. 23, no. 20, pp. 26800–26813, Oct. 2015.
[20] A. Tait, M. Nahmias, B. Shastri, and P. Prucnal, "Broadcast and weight: An integrated network for scalable photonic spike processing," *J. Lightw. Technol.*, vol. 32, no. 21, pp. 4029–4041, Nov. 2014.
[21] T. Do-Hong and P. Russer, "Signal processing for wideband array applications," *IEEE Microw. Mag.*, vol. 5, no. 1, pp. 57–67, Mar. 2004.